Int. J. Solids Structures Vol. 23, No. 9, pp. 1269–1283, 1987
Printed in Great Britain.

0020–7683/87 $3.00+ .00

THE EFFECT OF FIBER BREAKS AND ALIGNED PENNY-SHAPED CRACKS ON THE STIFFNESS AND ENERGY RELEASE RATES IN UNIDIRECTIONAL COMPOSITES

N. LAWS
Department of Mechanical Engineering, University of Pittsburgh, Pittsburgh, PA 15261, U.S.A.

and

G. J. DVORAK
Department of Civil Engineering, Rensselaer Polytechnic Institute, Troy, NY 12181, U.S.A.

(*Received* 4 *June* 1986; *in revised form* 11 *November* 1986)

Abstract—The loss of stiffness due to penny-shaped cracks associated with fiber breaks in a unidirectional composite is the main theme of the paper. Explicit results are given for the non-trivial Hashin–Shtrikman bound together with the estimates obtained from the self-consistent and differential schemes. In addition the paper contains some results on energy release rates for two different crack growth mechanisms. It is shown that, in theory, the differential scheme enjoys a distinguished position.

1. INTRODUCTION

This paper is mainly concerned with the changes of stiffness and strength of a unidirectional fiber-reinforced solid due to fiber breaks accompanied by penny-shaped cracks at the ends of the broken fibers.

The literature on the effect of crack distributions on the response of solids falls into two categories. First one can consider periodic distributions of cracks, see e.g. Delameter *et al.*[1]. Second, and this is by far the major part of the literature, one can consider random distributions of cracks. Within this second category, the pioneering paper is due to Budiansky and O'Connell[2], although a less general approach was given independently by Salganik[3]. The work of Budiansky and O'Connell[2] was especially directed at predicting the loss of stiffness of an isotropic solid due to a volume distribution of randomly oriented elliptical cracks—leading to isotropy of the cracked solid. Additional work on the effect of slit cracks on the stiffness of anisotropic solids has been given by Gottesman *et al.*[4], and by Laws and Dvorak[5, 6].

It is particularly relevant to the analysis of this paper to call attention to the work of Hoenig[7] who was the first to consider anisotropic distributions of cracks. In addition, it is important to recognize the contributions of Mura and Taya[8] and Taya[9] which were addressed to the problem of determining the effect of fiber breaks on the response of unidirectional fiber-reinforced materials.

In this paper we extend the work of various authors[7–9] in that we obtain self-consistent estimates for the reduction in stiffness of unidirectional composites containing penny-shaped cracks. In addition we obtain the only non-trivial Hashin–Shtrikman bound on the moduli of the cracked solid. We also derive the appropriate differential scheme model for the loss of stiffness.

We show how both the self-consistent and differential scheme results are entirely consistent with the Hashin–Shtrikman bound. Further we show explicitly that the results of Mura and Taya[8, 9] *coincide* with the Hashin–Shtrikman bound.

As a further illustration of the results presented herein, we pay brief attention to *isotropic* solids containing distributions of aligned penny-shaped cracks and amongst other things, recover some results first given by Hoenig[7]. The relevance of this analysis in the study of micro-cracking in ceramics is discussed by Laws and Brockenbrough[10].

Finally we investigate the influence of cracks on energy release rates. Here, we consider two distinct cases. First, we consider situations in which all cracks extend simultaneously. Second, we consider only one crack in the effective cracked solid. It turns out that the differential scheme enjoys a distinguished position as far as the evaluation of energy release rates is concerned. Whether or not this is of physical significance is an open question.

2. PHYSICAL MOTIVATION

Consider a unidirectional graphite–epoxy composite subject to loading parallel to the fibers. It is known that such composite specimens eventually suffer fiber breakage. The density of such fiber breaks can be quite large before final fracture occurs. At the end of each broken fiber, one usually finds penny-shaped cracks (whose normals are in the fiber direction). Under continued loading, these cracks may extend—see the discussion of Mura and Taya[8, 9] and the references contained therein.

In addition there is ample evidence that in cross-ply composite laminates, one often sees fiber breaks in the 0° plies at the end of transverse cracks in the 90° plies. Furthermore, some recent work by Laws and Brockenbrough[10] indicates the relevance of considering aligned penny-shaped micro-cracks in ceramics.

Another application arises in fibrous composites which can develop aligned matrix cracks on planes perpendicular to the fibers. Such cracks are confined to the matrix and do not extend through the fibers. They have been observed in 0° plies of cyclically loaded boron–aluminum laminates by Dvorak and Johnson[11].

It is, therefore, desirable that the effects of aligned penny-shaped cracks on the stiffness and strength of both composites and single phase materials be more fully understood.

3. ANALYSIS

In this section we present the mechanics of the effect of distributions of aligned penny-shaped cracks on the stiffness and strength of solids. For simplicity we shall discuss cracked composites by regarding the uncracked fibrous composite as an effective homogeneous material. This is, of course, commonplace in the theory of composites, but some further explanation is required here since the cracked composite will contain both long and short (broken) fibers.

Now Laws and McLaughlin[12], followed by Chou *et al.*[13], have quantified the effects of fiber aspect ratio on the overall moduli of aligned short fiber-reinforced composites. The general conclusion is that for aspect ratios greater than 100, say, the stiffness of the composite is insensitive to fiber length. Since the applications discussed in Section 2 all indicate broken fibers whose aspect ratios are much larger than 100, there is no loss of generality in considering only long fibers. If we interpret correctly, Taya[9] arrives at the same conclusion, by somewhat different methods.

In addition for transverse cracks in composite laminates the use of a model with cracks in an otherwise homogeneous solid is well established.

The notation and basic ideas presented here are taken directly from the work of Laws and Dvorak[5, 6]. Fourth-order tensors are denoted by upper case letters, e.g. L, Λ and symmetric second-order tensors are denoted by bold-face letters, e.g. $\boldsymbol{\varepsilon}$, $\boldsymbol{\sigma}$. The unit fourth-order tensor is denoted by I and the inverse of a non-singular fourth-order tensor A is denoted by A^{-1}.

Consider a linear elastic solid whose stress tensor, $\boldsymbol{\sigma}$, and strain tensor, $\boldsymbol{\varepsilon}$, are related through

$$\boldsymbol{\sigma} = L\boldsymbol{\varepsilon}, \qquad \boldsymbol{\varepsilon} = M\boldsymbol{\sigma}, \qquad LM = ML = I. \tag{1}$$

We use a standard 6×6 matrix notation for the stiffness tensor L and compliance tensor M. Since we are here concerned with materials which are at worst transversely isotropic with respect to the coordinate axis $0x_3$, it follows that eqns (1) may be written in the form

$$\begin{bmatrix}\sigma_1\\ \sigma_2\\ \sigma_3\\ \sigma_4\\ \sigma_5\\ \sigma_6\end{bmatrix} = \begin{bmatrix} L_{11} & L_{12} & L_{13} & 0 & 0 & 0\\ & L_{11} & L_{13} & 0 & 0 & 0\\ & & L_{33} & 0 & 0 & 0\\ & & & L_{44} & 0 & 0\\ & \text{SYM} & & & L_{44} & 0\\ & & & & & L_{66}\end{bmatrix} \begin{bmatrix}\varepsilon_1\\ \varepsilon_2\\ \varepsilon_3\\ \varepsilon_4\\ \varepsilon_5\\ \varepsilon_6\end{bmatrix}. \tag{2}$$

$$\begin{bmatrix}\varepsilon_1\\ \varepsilon_2\\ \varepsilon_3\\ \varepsilon_4\\ \varepsilon_5\\ \varepsilon_6\end{bmatrix} = \begin{bmatrix} M_{11} & M_{12} & M_{13} & 0 & 0 & 0\\ & M_{11} & M_{13} & 0 & 0 & 0\\ & & M_{33} & 0 & 0 & 0\\ & & & M_{44} & 0 & 0\\ & \text{SYM} & & & M_{44} & 0\\ & & & & & M_{66}\end{bmatrix} \begin{bmatrix}\sigma_1\\ \sigma_2\\ \sigma_3\\ \sigma_4\\ \sigma_5\\ \sigma_6\end{bmatrix}. \tag{3}$$

where

$$L_{66} = \tfrac{1}{2}(L_{11} - L_{12}), \qquad M_{66} = 2(M_{11} - M_{12}). \tag{4}$$

We use the suffix 0 to refer to the initial uncracked solid. Thus, for example L_0 is the stiffness of the uncracked solid, whereas L is the stiffness of the cracked solid. The volume concentration of cavities is denoted by c.

It is convenient, but not essential, to develop the theory by considering a family of aligned spheroidal cavities in a transversely isotropic matrix. A typical spheroid is taken to be

$$\frac{x_1^2}{a^2} + \frac{x_2^2}{a^2} + \frac{x_3^2}{b^2} = 1. \tag{5}$$

In addition we suppose all cavities to be of equal size. This assumption is *not* essential as far as theory is concerned, but may well be essential in any application to penny-shaped cracks at the ends of broken fibers in a unidirectional composite. Ultimately we will obtain the required results for aligned penny-shaped cracks by allowing the aspect ratio

$$\varepsilon = b/a \tag{6}$$

to approach zero.

Many methods have been proposed to predict the effect of reinforcement on the effective moduli of composites. It is not our purpose here to give a critical survey of the various methods. Rather, we give the required formula for the Hashin–Shtrikman bounds, the self-consistent method and the differential scheme.

In order to get the Hashin–Shtrikman bounds we refer to the work by Willis[14]. We assume that the cavities are randomly located so that the cracked solid exhibits overall transverse isotropy. Since this envisaged distribution of oblate spheroidal cavities will conform to the statistics assumed by Willis[14], it follows that the overall compliance of the cracked composite must satisfy

$$M \geqslant M_0 + \frac{c}{1-c} Q_0^{-1}. \tag{7}$$

Here Q_0 is a tensor which depends on the uncracked compliance M_0 and the aspect ratio ε. The components of Q_0 can be found explicitly, see Laws and McLaughlin[12] or Laws[15].

The right-hand side of inequality (7) is the Hashin–Shtrikman lower bound for M, denoted here by M^-

$$M^- = M_0 + \frac{c}{1-c} Q_0^{-1}. \tag{8}$$

Since the damaged material contains cavities the Hashin–Shtrikman upper bound for M is here infinite.

Next we recall that the self-consistent estimate is given by Laws *et al.*[5] as

$$M = M_0 + cQ^{-1}. \tag{9}$$

Finally, it is easy to read off the differential scheme estimate from the work of McLaughlin[16]

$$\frac{dM}{dc} = \frac{1}{1-c} Q^{-1} \tag{10}$$

with

$$M = M_0 \quad \text{when} \quad c = 0. \tag{11}$$

In terms of the stiffness tensor L it is easy to show that the upper bound L^+ is given by

$$L^+ = \left[M_0 + \frac{c}{1-c} Q_0^{-1} \right]^{-1}. \tag{12}$$

Also the self-consistent result is

$$L = L_0 [I + cQ^{-1} L_0]^{-1} \tag{13}$$

whereas the differential scheme gives

$$\frac{dL}{dc} = -\frac{1}{1-c} LQ^{-1} L \tag{14}$$

with

$$L = L_0 \quad \text{when} \quad c = 0. \tag{15}$$

We now obtain the required results for penny-shaped cracks by proceeding to the limit as $\varepsilon \to 0$. Let η be the number of cracks per unit volume then

$$c = \frac{4}{3} \pi \eta a^3 \varepsilon$$

$$= \frac{\pi}{6} \alpha \varepsilon$$

where the crack density parameter α is defined by

$$\alpha = 8 \eta a^3. \tag{16}$$

Note that the crack density parameter is *not* the same as the crack density parameter

introduced by Budiansky and O'Connell[2]. The choice of eqn (16) is motivated by the fact that $\alpha = 1$ corresponds to an average of one crack of diameter $2a$ in each cube of side $2a$.

In applications of the theory to composites reinforced by aligned continuous fibers, the crack can, in the first instance, be visualized as a fiber break which has extended into the surrounding matrix and has been arrested by adjacent unbroken fibers. This crack is then regarded as a crack in an effective composite medium. For practical purposes it is desirable to relate the radius of this crack to the fiber radius, r_f, and the fiber volume fraction, v_f. Estimates can be obtained in various ways. For example if the microstructure is such that the fibers are located in a close packed hexagonal array and that failure of one fiber creates a crack which extends through the matrix until it reaches the surfaces of neighboring fibers, then the resulting penny-shaped crack has radius

$$a = r_f\left\{\left(\frac{2\pi}{v_f}\right)^{1/2} 3^{-1/4} - 1\right\}. \tag{17}$$

In the same spirit one obtains the estimate

$$a = r_f\left\{\left(\frac{\pi}{v_f}\right)^{1/2} - 1\right\} \tag{18}$$

for a square array. For typical volume fractions occurring in practice the hexagonal array estimate exceeds the square array estimate by about 13%.

As noted by Eshelby[17] in the isotropic case, and by Hoenig[7] and Laws[15] for orthotropic materials, the limit as ε approaches zero needs to be handled with care. The essential point here is that whereas Q becomes singular, the product εQ^{-1} remains finite. Thus let

$$\lim_{\varepsilon \to 0} \varepsilon Q^{-1} = \Lambda$$

with an analogous definition for Λ_0. The components of Λ are given in the Appendix.

In the limit of aligned penny-shaped cracks it now follows from eqn (8) that

$$M^- = M_0 + \frac{\pi}{6}\alpha\Lambda_0. \tag{19}$$

Further, the self-consistent estimate is obtained from

$$M = M_0 + \frac{\pi}{6}\alpha\Lambda \tag{20}$$

whereas the differential scheme yields

$$\frac{dM}{d\alpha} = \frac{\pi}{6}\Lambda. \tag{21}$$

The dual formulae for the stiffness tensor are

$$L^+ = L_0\left[I + \frac{\pi}{6}\alpha\Lambda_0 L_0\right]^{-1} \tag{22}$$

the self-consistent result being

$$L = L_0\left[I + \frac{\pi}{6}\alpha\Lambda L_0\right]^{-1} \tag{23}$$

and the differential scheme giving

$$\frac{\mathrm{d}L}{\mathrm{d}\alpha} = -\frac{\pi}{6}L\Lambda L. \tag{24}$$

Since the only non-zero components of Λ (shown in the Appendix) are Λ_{33} and Λ_{44} $(= \Lambda_{55})$ it follows from eqns (20) and (21) that only M_{33} and M_{44} $(= M_{55})$ are predicted to change. This is, of course, only to be expected.

It is instructive to consider the rather special case when the uncracked body is *isotropic*. Thus let E_0, ν_0 be respectively the initial Young's modulus and Poisson's ratio. Then, from the Appendix, we see that

$$\Lambda^0_{33} = \frac{4(1-\nu_0^2)}{\pi E_0}$$

$$\Lambda^0_{44} = \frac{8(1-\nu_0^2)}{\pi E_0(2-\nu_0)}.$$

With the help of a standard notation

$$M_{33} = \frac{1}{E_L}, \qquad M_{44} = \frac{1}{G_L}$$

it now follows from eqn (19) that

$$\frac{E_L^+}{E_0} = \frac{1}{\frac{1}{2} + \frac{2}{3}\alpha(1-\nu_0^2)} \tag{25}$$

$$\frac{G_L^+}{G_0} = \frac{1}{1 + \frac{2}{3}\alpha(1-\nu_0)/(2-\nu_0)}. \tag{26}$$

We emphasize that eqn (25) is *precisely* the formula given by Taya[9]. Hence we see that the Mori–Tanaka[19] back-stress analysis, which is used by Taya[9], yields the non-trivial Hashin–Shtrikman bound. It is noteworthy that it is possible to show that the assumptions of the Mori–Tanaka[19] back-stress analysis lead to formulae which are coincident with the Hashin–Shtrikman bounds in other situations—but we do not include details here.

We remark that there is no difficulty in obtaining eqns (19)–(21) by direct methods instead of using an argument based on cavities. In fact Gottesman *et al.*[4] have given such an argument to obtain the bounds and self-consistent results for a solid with slit cracks. We note that the fully general analysis is given by Laws and Brockenbrough[10].

Numerical results can be found from eqns (19) to (21) or from eqns (22) to (24). In practice, we have found it easier to evaluate the compliances from eqns (19) to (21) and then to determine the stiffness, when required, by matrix inversion.

For the most part we present results for the loss in stiffness of unidirectional fiber-reinforced materials containing a distribution of penny-shaped cracks with common orientation perpendicular to the fiber direction. In other words we attempt to model the loss of stiffness of unidirectional fiber-reinforced materials due to fiber breaks. Data for the uncracked composite is taken directly from Table 2 of the paper by Dvorak *et al.*[6] which is for a T300/5208 graphite–epoxy system with volume fractions $c_f = 0.2, 0.4, 0.6$. As noted earlier the only compliances which change are M_{33}, M_{44} $(= M_{55})$. In Figs 1 and 2 we give

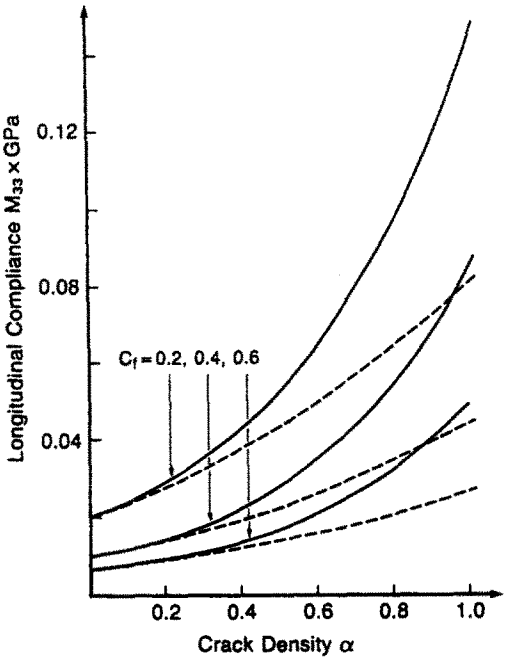

Fig. 1. Longitudinal compliance for various T300/5208 systems: (a) s.c.m. ———; (b) d.s. – – – –.

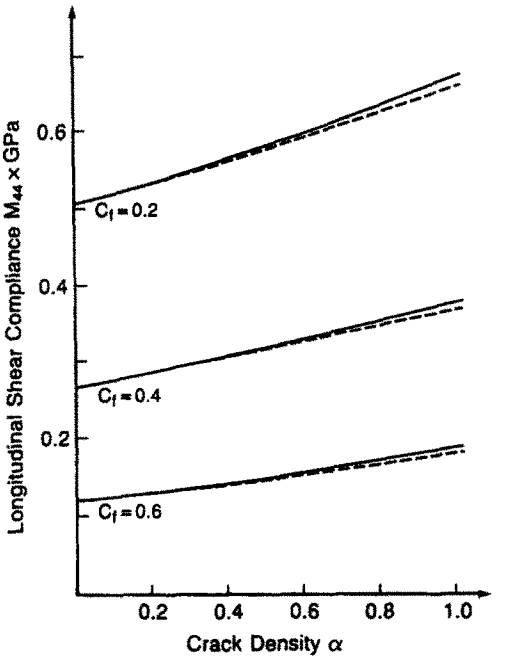

Fig. 2. Longitudinal shear compliance for various T300/5208 systems: (a) s.c.m. ———; (b) d.s. – – – –.

the self-consistent and differential scheme predictions for these two compliances. There is no need to display the Hashin–Shtrikman bound since it coincides with the common tangent at $\alpha = 0$. We observe that for each value of c_f the self-consistent result is always greater than the differential scheme result. For small α (<0.1 say) the two results for M_{33} are coincident and equal to the Hashin–Shtrikman bound. On the other hand, we see from Fig. 2 that there is virtually no difference between the self-consistent, the differential scheme and the Hashin–Shtrikman results for M_{44} for $\alpha < 0.5$. Thus for practical purposes it suffices to take

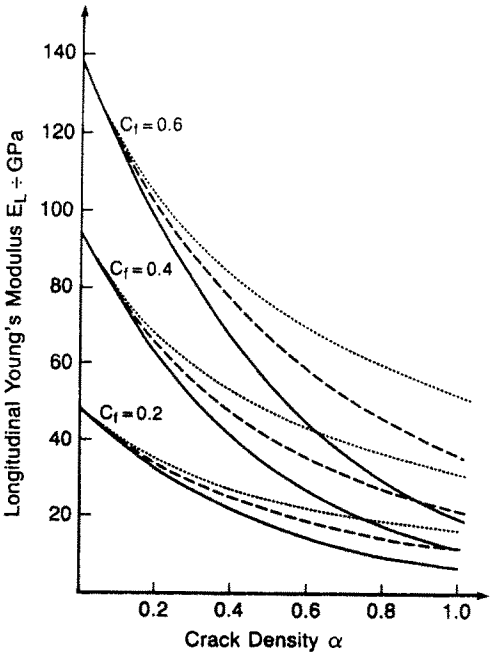

Fig. 3. Longitudinal Young's modulus for various T300/5208 systems: (a) bound ———; (b) s.c.m. – – – –; (c) d.s. ·····.

$$M_{44} = M_{44}^{-}$$
$$= M_{44}^{0} + \frac{\pi}{6}\alpha\Lambda_{44}^{0}$$

where Λ_{44}^{0} can be found from the formulae given in the Appendix.

The presentation of the results is sometimes clearer when we use the respective Young's moduli, Poisson's ratios and shear moduli. Thus we write

$$M = \begin{bmatrix} \frac{1}{E_T} & -\frac{\nu_{TT}}{E_T} & -\frac{\nu_{TL}}{E_T} & 0 & 0 & 0 \\ -\frac{\nu_{TT}}{E_T} & \frac{1}{E_T} & -\frac{\nu_{TL}}{E_T} & 0 & 0 & 0 \\ -\frac{\nu_{LT}}{E_L} & -\frac{\nu_{LT}}{E_L} & \frac{1}{E_L} & 0 & 0 & 0 \\ 0 & 0 & 0 & \frac{1}{G_L} & 0 & 0 \\ 0 & 0 & 0 & 0 & \frac{1}{G_L} & 0 \\ 0 & 0 & 0 & 0 & 0 & \frac{1}{G_T} \end{bmatrix}.$$

Since the only changed compliances are M_{33}, M_{44} and M_{55}, it follows that E_T and G_T are not changed by the introduction of cracks. Also the only Poisson's ratio which is changed is ν_{LT} (for transverse contraction due to longitudinal extension). Results showing the reduction of E_L and G_L are given in Figs 3 and 4, respectively. In both cases the Hashin–Shtrikman bound is nontrivial; actually

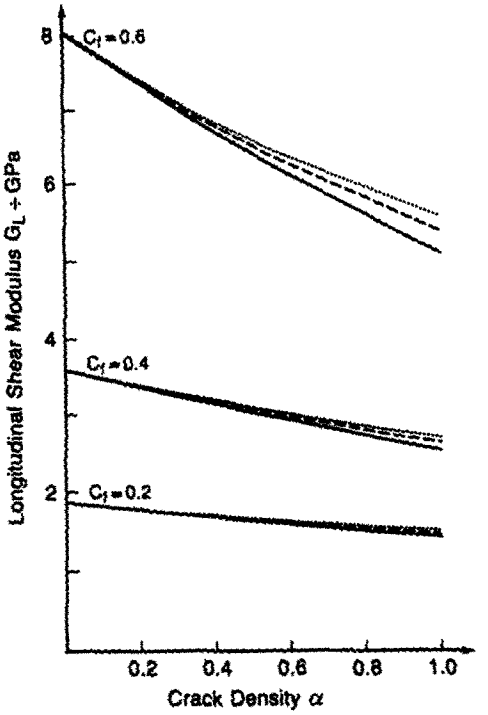

Fig. 4. Longitudinal shear modulus for various T300/5208 systems: (a) bound ———; (b) s.c.m. – – –; (c) d.s. ·····.

$$\frac{E_L^+}{E_L^0} = \left(1 + \frac{\pi}{6}\alpha E_L^0 \Lambda_{33}^0\right)^{-1}$$

$$\frac{G_L^+}{G_L^0} = \left(1 + \frac{\pi}{6}\alpha G_L^0 \Lambda_{44}^0\right)^{-1}.$$

We note that the self-consistent estimate for both E_L and G_L is always lower than the differential scheme result. Clearly both results are consistent with the Hashin–Shtrikman bound.

As for the reduction in ν_{LT} we note that since $M_{13} = M_{13}^0$ and $M_{13} = M_{31}$, it follows that

$$\frac{\nu_{LT}}{\nu_{LT}^0} = \frac{E_L}{E_L^0}.$$

Hence the fractional reduction of ν_{LT} is equal to the fractional reduction of E_L. Also the actual reduction in ν_{LT} can be found from the reduction of E_L merely by a change in scale. For clarity Figs 5 and 6 display only the fractional reduction for E_L and G_L when $c_f = 0.6$. We remark that the appropriate curves for $c_f = 0.2$ and 0.4 are *almost* indistinguishable from the curves indicated in Figs 5 and 6. By way of comparison Figs 7 and 8 show the fractional reduction of E_L and G_L for an *isotropic* material with Poisson's ratio $\nu_0 = 0.3$. Two remarks are in order. First the fractional reduction curves indicated in Figs 6 and 7 are insensitive to the choice of Poisson's ratio: $0.2 \leqslant \nu_0 \leqslant 0.4$. Second the fractional reductions indicated in Figs 5 and 6 compared with those in Figs 7 and 8 show that there is no possibility of constructing "master curves" for anisotropic materials.

4. ENERGY RELEASE RATES

In this section we calculate energy release rates for two different mechanisms of crack growth. First, we consider a solid which contains a family of cracks each of radius a and

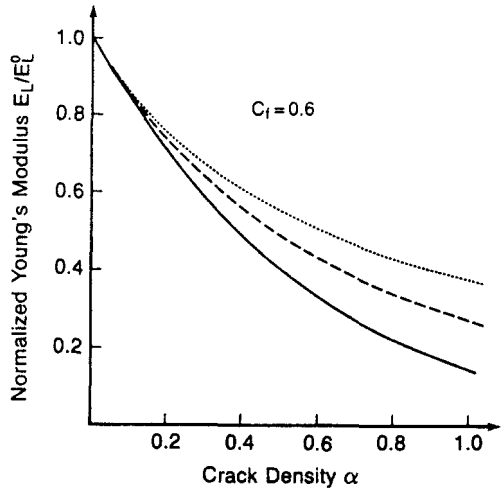

Fig. 5. Normalized longitudinal Young's modulus for the T300/5208 system with $c_f = 0.6$: (a) bound ———; (b) s.c.m. – – – –; (c) d.s. · · · · · · ·.

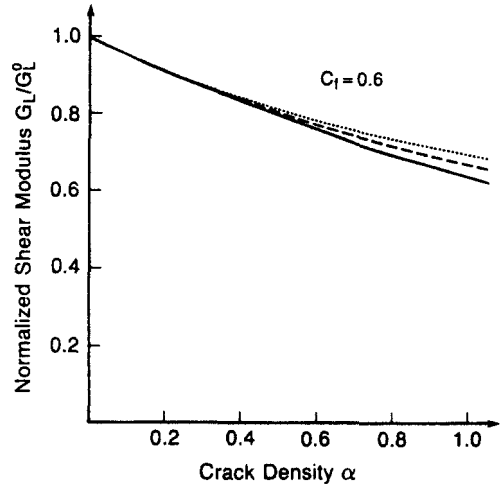

Fig. 6. Normalized longitudinal shear modulus for the T300/5208 system with $c_f = 0.6$: (a) bound ———; (b) s.c.m. – – – –; (c) d.s. · · · · · · ·.

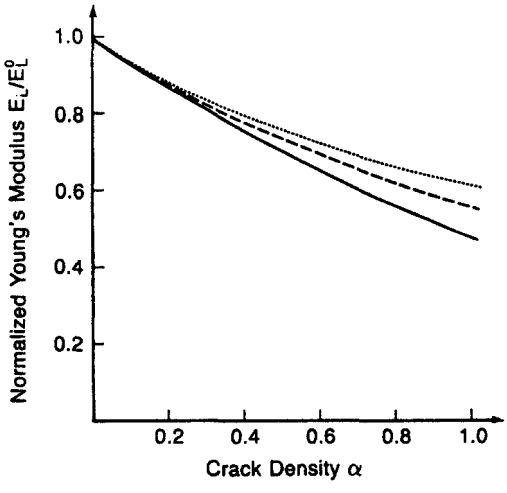

Fig. 7. Normalized longitudinal Young's modulus for isotropic materials with Poisson's ratio = 0.3: (a) bound ———; (b) s.c.m. – – – –; (c) d.s. · · · · · · ·.

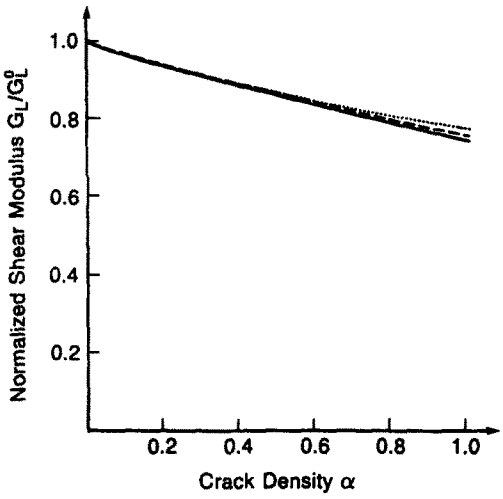

Fig. 8. Normalized longitudinal shear modulus for isotropic materials with Poisson's ratio = 0.3: (a) bound ———; (b) s.c.m. – – – –; (c) d.s. · · · · · · ·.

allow each crack to extend by the same amount. Second, we consider a single penny-shaped crack in an otherwise homogeneous (cracked) solid. We show, *inter alia*, that the differential scheme enjoys a peculiar status in that it predicts equality of the two energy release rates.

Thus we first consider a solid containing a family of aligned penny-shaped cracks each of radius a. The corresponding crack density is α. The solid is subject to macroscopically uniform loading with applied stress $\bar{\sigma}$, which is also the average stress. All cracks are assumed to be open. The *total energy* of the cracked solid is

$$E(\alpha) = \frac{1}{2}\int_V \boldsymbol{\sigma}\cdot\boldsymbol{\varepsilon}\,\mathrm{d}V - \int_S \mathbf{T}\cdot\mathbf{u}\,\mathrm{d}S \tag{27}$$

where $\mathbf{T}$, $\mathbf{u}$ are respectively the tractions and displacements on the boundary S. It is easy to show that eqn (27) may be rewritten in the form

$$\begin{aligned} E(\alpha) &= -\tfrac{1}{2}V\bar{\sigma}\cdot M(\alpha)\bar{\sigma} \qquad \text{when } \alpha \neq 0, \\ E_0 &= -\tfrac{1}{2}V\bar{\sigma}\cdot M_0\bar{\sigma} \qquad \text{when } \alpha = 0. \end{aligned} \tag{28}$$

Thus the total energy released by the introduction of cracks is $(E_0 - E(\alpha))$. Accordingly the energy released by *each* crack, $W(\alpha)$, is given by

$$\begin{aligned} W(\alpha) &= \frac{E_0 - E(\alpha)}{\eta V} \\ &= \frac{1}{2\eta}\bar{\sigma}\cdot[M(\alpha) - M_0]\bar{\sigma}. \end{aligned} \tag{29}$$

Suppose now that each crack extends from radius a to radius $(a+\delta a)$ while the *total number of cracks remains constant*. This corresponds to an increase in crack density from α to $(\alpha+\delta\alpha)$. The crack extension force, or energy release rate per unit length, G_A, of each crack is given by

$$G_A = \frac{1}{2\pi a}\frac{\partial W}{\partial \alpha}\frac{\mathrm{d}\alpha}{\mathrm{d}a}. \tag{30}$$

Here the subscript A is used to signify that G_A is the energy release rate of each crack when *all* cracks extend simultaneously. From eqn (16)

$$\frac{d\alpha}{da} = 24\eta a^2$$

so from eqns (29) and (30)

$$G_A = \frac{6a}{\pi}\bar{\sigma}\cdot\frac{\partial M}{\partial\alpha}\bar{\sigma}. \tag{31}$$

The lower bound M^- in eqn (19) gives

$$G_A^- = a\bar{\sigma}\cdot\Lambda_0\bar{\sigma}$$

while the self-consistent estimate of M in eqn (20) yields

$$G_A = a\bar{\sigma}\cdot\left(\Lambda+\alpha\frac{d\Lambda}{d\alpha}\right)\bar{\sigma}$$

and the differential scheme result, eqn (21), gives

$$G_A = a\bar{\sigma}\cdot\Lambda\bar{\sigma}.$$

Next we focus on a single penny-shaped crack in the cracked solid. We now regard the cracked solid as a homogeneous medium with effective compliance $M(\alpha)$. Only one crack is now present in this effective medium and we wish to determine the energy release rate, G_S, for extension of this *single* crack.

In these circumstances we can use the results of Laws[15] to obtain the required energy released by extension of this single crack of radius a

$$\mathscr{E}(a) = \tfrac{2}{3}\pi a^3\bar{\sigma}\cdot\Lambda\bar{\sigma}.$$

Hence

$$G_S = \frac{1}{2\pi a}\frac{\partial\mathscr{E}}{\partial a} = a\bar{\sigma}\cdot\Lambda\bar{\sigma}. \tag{32}$$

We emphasize that different models give rise to different values of M. Since the components of Λ are given in terms of the components of M by the formulae of the Appendix, it follows that each of the three models gives rise to a different value of Λ and hence of G_S.

Whether we consider all cracks simultaneously growing in self-similar fashion or a single growing crack, it is clear that both G_A and G_S are *average* crack extension forces. Of course if we are considering crack extension in a *single phase* brittle solid there is no conceptual problem. However, in the case when the cracks are located in an effective composite matrix some further comments are in order. Thus consider an arbitrary growing penny-shaped crack in a unidirectional fiber-reinforced composite—with the plane of the crack perpendicular to the fiber direction. In the first place this crack will arise from a fiber break followed by extension through the matrix until the circumferential crack tip reaches neighboring fibers. If there is further growth then part of the crack tip must lie in the matrix material whereas the remainder must lie in the fibers. Since here we consider cracks in an effective solid it is clear that the energy release rates G_A and G_S do not apply when the crack radius is smaller than the value given in eqn (17) or eqn (18). However, for subsequent growth an *average* crack extension force is precisely the quantity which is demanded by the physics of the problem.

Taya[9] has reported some work on the second case (G_S) but his work appears to have little in common with the work described here.

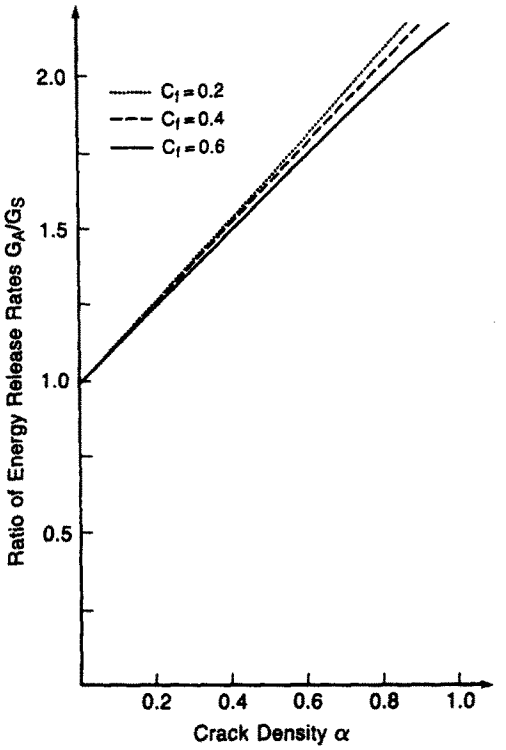

Fig. 9. Ratio of energy release rates for various T300/5208 systems according to s.c.m.

From eqns (21), (29) and (30) we obtain the surprising result that the differential scheme predicts that $G_A = G_S$. Thus the differential scheme can provide a useful border between those models which predict G_A to be greater or smaller than G_S. However, one ought to bear in mind that there is no *a priori* reason why a particular model should not give $G_A > G_S$ for small α and yet $G_A < G_S$ for large α.

Since a general analysis of eqns (29) and (30) is complicated by the fact that both refer to mixed mode loading, we concentrate on mode I loading in which the only non-zero applied stress is $\bar{\sigma}_{33}$. From eqns (31) and (32) we have

$$\frac{G_A}{G_S} = \frac{6}{\pi} \frac{\mathrm{d}M_{33}/\mathrm{d}\alpha}{\Lambda_{33}}.$$

It is perhaps useful to emphasize here that both G_A and G_S depend upon crack density. This may be contrasted with the usual situation in fracture mechanics wherein a single crack extends in a material of fixed properties. Nevertheless we see from eqns (31) and (32) that if $G_A/G_S \geqslant 1$ extension of all cracks is indicated rather than extension of a single crack. When $G_A/G_S < 1$ the opposite conclusion applies.

Numerical results can be obtained for the T300/5208 graphite–epoxy systems considered earlier. In particular Fig. 9 shows the self-consistent and (trivially) the differential scheme estimates for G_A/G_S. Since $G_A/G_S \geqslant 1$ both models suggest extension of all cracks. By way of comparison Fig. 10 shows the results for initially isotropic solids in which case the value of G_A/G_S is insensitive to the choice of initial Poisson's ratio in the range $0.2 \leqslant \nu_0 \leqslant 0.4$.

A further general conclusion on energy release rates for a *single* crack can be obtained from eqn (30) and the results of Section 3. For simplicity consider the mixed mode loading $\bar{\sigma}_{33} \neq 0$, $\bar{\sigma}_{23} \neq 0$ so that eqn (30) reduces to

$$G_S = a\Lambda_{33}(\bar{\sigma}_{33})^2 + a\Lambda_{44}(\bar{\sigma}_{23})^2.$$

Thus Λ_{33} and Λ_{44} may be interpreted as energy release rate factors. Indeed Figs 11 and 12

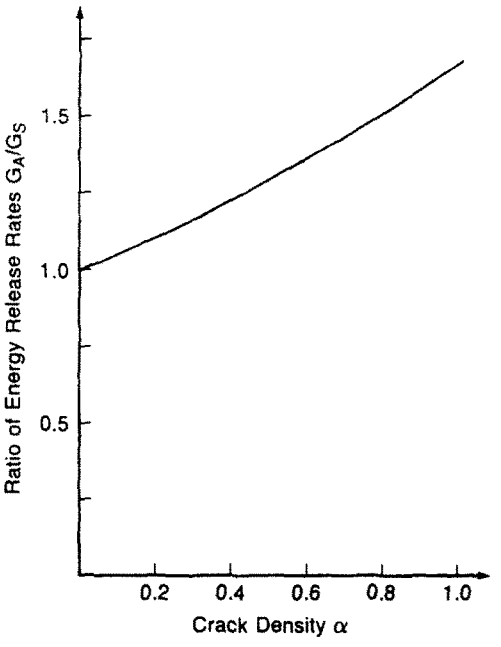

Fig. 10. Ratio of energy release rates for isotropic materials with Poisson's ratio = 0.3 according to s.c.m.

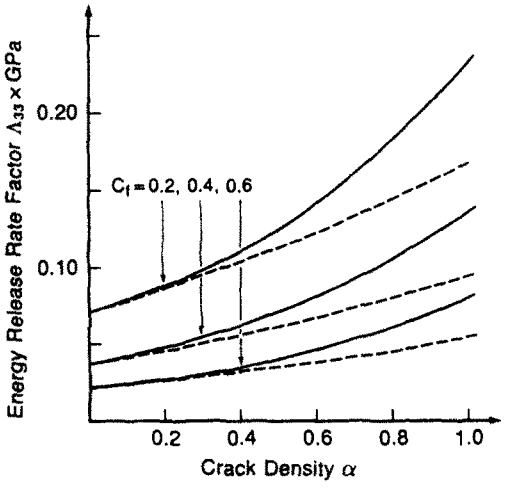

Fig. 11. Energy release rate factor for various T300/5208 systems: (a) s.c.m. ———, (b) d.s. – – – –.

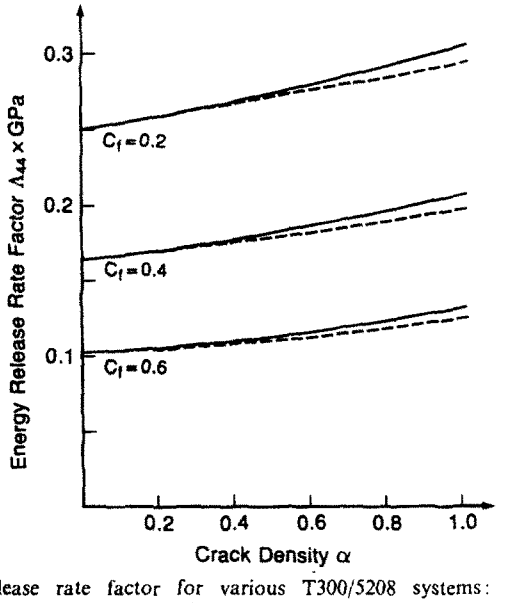

Fig. 12. Energy release rate factor for various T300/5208 systems: (a) s.c.m. ———; (b) d.s. – – – –.

contain the self-consistent and differential scheme results for Λ_{33} and Λ_{44} for the T300/5208 systems considered earlier. It is clear that both models predict that at fixed crack density, Λ_{33} and Λ_{44} decrease as the volume fraction of fiber increases. Hence G_S decreases as the volume fraction of fiber increases in agreement with some results of Taya[9]. Further it is evident that, for fixed c_f, G_S increases with α.

Finally, we note that in the fibrous composite medium the crack density will increase gradually under incremental load, as a result of fiber breaks at randomly distributed locations. Each new crack will require for its formation at least the same amount of crack energy as the first crack, i.e. $W(\alpha) \geqslant W_0$. Equation (29) indicates that this will be the case for all models considered herein. Therefore, progressive cracking is governed by spatial variation of fiber strength; sufficient crack energy is available for each fiber break to produce a new crack.

Acknowledgement—This work was supported by a grant from the Air Force Office of Scientific Research.

REFERENCES

1. W. R. Delameter, G. Herrmann and D. M. Barnett, *J. Appl. Mech.* **42**, 74 (1975); **44**, 190 (1977).
2. B. Budiansky and R. J. O'Connell, *Int. J. Solids Structures* **12**, 81 (1976).
3. R. L. Salganik, *Mekh. Tverd. Tela* **4**, 149 (1973).
4. T. Gottesman, Z. Hashin and M. A. Brull, *Advances in Composite Materials* (Edited by A. R. Bunsell, A. Martrenchar, D. Menkes, C. Bathias and G. Verchery), p. 749. Pergamon Press, Oxford (1980).
5. N. Laws, G. J. Dvorak and M. Hejazi, *Mech. Mater.* **2**, 123 (1983).
6. G. J. Dvorak, N. Laws and M. Hejazi, *J. Composite Mater.* **19**, 216 (1985).
7. A. Hoenig, *Int. J. Solids Structures* **15**, 137 (1979).
8. T. Mura and M. Taya, *J. Appl. Mech.* **48**, 361 (1981).
9. M. Taya, *J. Composite Mater.* **15**, 198 (1981).
10. N. Laws and J. R. Brockenbrough, *Int. J. Solids Structures* **23**, 1247 (1987).
11. G. J. Dvorak and W. S. Johnson, *Int. J. Fracture* **16**, 585 (1980).
12. N. Laws and R. McLaughlin, *J. Mech. Phys. Solids* **27**, 1 (1979).
13. T. W. Chou, S. Nomura and M. Taya, *J. Composite Mater.* **14**, 178 (1980).
14. J. R. Willis, *J. Mech. Phys. Solids* **25**, 185 (1977).
15. N. Laws, *Mech. Mater.* **4**, 209 (1985).
16. R. McLaughlin, *Int. J. Engng Sci.* **15**, 237 (1977).
17. J. D. Eshelby, *Proc. R. Soc. Lond.* **A241**, 376 (1957).
18. N. Laws, *Phil. Mag.* **36**, 367 (1977).
19. T. Mori and K. Tanaka, *Acta Metall.* **21**, 571 (1973).

APPENDIX

For completeness we give here the formulae for the non-zero components of the Λ tensor, defined in eqn (18), for a penny-shaped crack in a transversely isotropic material. The crack lies in a plane normal to the axis of transverse isotropy. As is shown by Laws[15]

$$\Lambda_{33} = \frac{2\gamma_1\gamma_2(\gamma_1+\gamma_2)}{\pi}\frac{M_{11}^2 - M_{12}^2}{M_{11}}$$

$$\Lambda_{44} = \Lambda_{55} = \frac{4(\gamma_1+\gamma_2)(M_{11}^2 - M_{12}^2)(2M_{44})^{1/2}}{\pi\{M_{11}(2M_{44})^{1/2} + (\gamma_1+\gamma_2)(M_{11}+M_{12})(M_{11}-M_{12})^{1/2}\}}$$

where γ_1^2 and γ_2^2 are the roots of

$$(M_{11}^2 - M_{12}^2)x^2 - [M_{11}M_{44} + 2M_{13}(M_{11}-M_{12})]x + M_{11}M_{33} - M_{13}^2 = 0.$$

When the material is isotropic with Young's modulus E and Poisson's ratio ν, it is easy to see that $\gamma_1 = \gamma_2 = 1$. Hence

$$\Lambda_{33} = \frac{4(1-\nu^2)}{\pi E}$$

$$\Lambda_{44} = \frac{8(1-\nu^2)}{\pi E(2-\nu)}.$$

These results are in complete agreement with those of Eshelby[17].